CFD Simulation Verification Processes at Planing Hulls using An Interceptor

Budi Utomo[1], S Samuel[2] [*], Serliana Yulianti[2], Good Rindo[3], Muhammad Iqbal[4], Abubakar Fathuddiin[5]

[1] Marine Construction Engineering Technology, Vocational School, Diponegoro University, Semarang 50275, Indonesia
[2] Department of Naval Architecture, Faculty of Engineering, Diponegoro University, Semarang 50275, Indonesia
[3] Department Systems and Naval Mechatronic Engineering, National Cheng Kung University, University road, Tainan city 701, Taiwan
[4] Department of Naval Architecture, Ocean, and Marine Engineering, University of Strathclyde, Glasgow, UK
[5] Blue Gulf Cat, Sheikh Rashid bin Saeed St, Abu Dhabi, 41655, United Arab Emirates
[*] Corresponding Author : samuel@ft.undip.ac.id

Article Info

Abstract

Experimental test is one of the methods for predicting drag ships using towing tank. This method has a good level of accuracy but requires quite complex equipment and costs. With the advancing technology of computing, the CFD method has emerged as an alternative for problem-solving, especially in hydrodynamics analysis. This study aims to ensure the accuracy of Computational Fluid dynamics (CFD) by verifying experimental data on high-speed vessel using an interceptor. The Interceptor system generates a hydrodynamic lift force by intercepting the flow of water under the hull. Comparison of experimental results and numerical simulations will involve analysis of drag, heave and trim. Numerical simulations were carried out using ITTC recommendations as testing standards. This research uses the grid independence study method to ensure the accuracy of the mesh. CFD simulations were carried out using the overset mesh method and the k-epsilon to solve turbulence flow. The Dynamic Fluid Body Interaction (DFBI) module is employed to resolve the dynamic motion of the ship in order to assess hull movements based on by fluid forces and moments. There can be two degrees of freedom in the heave and pitch directions. All simulations are performed in calm water condition. Verification is carried out by reviewing the condition of the ship without an interceptor and with an interceptor. 100% stroke and 60% interceptor were used as variations of the verification of this study. The results of this study indicate that the CFD analysis has been verified by the experimental method with a maximum error range of 10.7%. Planing hull is a type of fast ship that has quite complex hydrodynamic characteristics. This study also shows that the use of interceptors is proven to improve the performance of the planing hull ship.

1. Introduction

Due to their motions, planing hulls present one of the most challenging issues in naval architecture, making hydrodynamic calculations and hull optimization more challenging. Researchers have made an effort experimental and computational approaches, with many assumptions. A planing hull that isn't moving forward floats in water because of the fluid's hydrostatic lift, or buoyancy.

A high-speed vessel with zero speed floats in water due to the fluid's hydrostatic force, also known as buoyancy. When it begins to move, the hull's geometry contributes to the generation of hydrodynamic force. The hull body experiences force from the fluid, creating a moment about the hull's centre of gravity that assists the vessel in rising above the water and producing dynamic force.

Savitsky was one of the first people to succeed in formulating and generalizing the motions of the hull (trim) and the drag (total resistance) it encounters in the flow [1]. In the Savitsky calculation method it is observed that if there is an increase in trim, the instability and resistance will increase. To solve this problem, one of the studies that have been carried out is the use of pneumatic trim tabs. With a mathematical model for the configuration of the pneumatic actuator system and control system design, pneumatic trim tabs are proven to be effective in reducing trim and even improving the performance of ship planing craft [2]. One alternative solution to control trim is to apply an interceptor. In another study, it was shown that the interceptor produces a positive and negative lifting force as a control force in the opposite direction so that the ship's motion becomes better [3]. The combination of trim tabs and interceptors is reported that interceptors have a better effect than trim tabs on the distribution of pressure area on the stern of the ship, thus creating a more effective interceptor moment to reduce

trim [4]. Investigations on fast boats show that the interceptor can increase the pressure and lift force followed by a reduction in the trim angle [5]. Studies on interceptors under regular head waves show that interceptors can reduce heave motion by 16% to 18% at Froude number 1.78 [6]. In addition, the interceptor will show different performance when using different strokes [7].

Savitsky formulated a formula that became a reference for research to predict drag on high speed vessel with an empirical approach [8]. However, as computing progressed, the Savitsky method had its limitations when studying complex ship geometries. Experimental research was conducted by Kim et al to review some of the complicated ship geometries [9]. The experimental method has high accuracy, but requires a lot of preparation, time and high costs during testing.

The other alternative is the numerical computation method. Although still being developed, the CFD method can also reduce research time and costs. Seeing the current development of computing, the Navier-Stokes equation is used as the basis for solving hydrodynamic problems in fluid flow. Research conducted by Yousefi et al discusses several methods, approaches, commercial CFD software related to ship planing hull. In this study, there are three methods that can be used to predict ship resistance, namely Finite Volume Method (FVM), Finite Element Method (FEM) and Boundary Element Method (BEM). FVM is the most widely used method to predict ship planing hull characteristics because of its better accuracy [10]. FEM research was successfully conducted in 2015 to evaluate catamaran resistance [11]. The research was continued by modifying the addition of a centerbulb to reduce the total resistance [12]. Sukas et al conducted research using a planing hull ship using the CFD method and compared it with the experimental results [13].

Several studies showed good results, Brizzola and Serra compared the CFD simulation results with the experimental data of Savitksy and Shepherd and acknowledged that CFD was able to provide good accuracy [14]. Hey et al performed a numerical analysis of unsteady flow on prismatic vessels [15]. In addition, experimental research shows the inaccuracy of calculations due to certain factors. Kim et al's experiment resulted in a resonant frequency correction of up to 70% due to the effect of counterbalanced in wavy conditions [9]. Another study revealed that the limitations of CFD at high FR rates can cause numerical ventilation problems (NPV) [16]. Wheeler et al. also discussed the validation of fast boats, the results of CFD simulations reported that several numerical analysis approaches showed differences at high speeds [17].

Some of the studies above prove the ability of CFD to be another alternative, but other studies also state the limitations of CFD in predicting ship resistance. The advantage of CFD is that it is easy to modify the shape and dimensions of an object, such as the application of an interceptor. In addition, CFD can save space and time, we can easily see and show phenomena that occur such as pressure, wave pattern, trim angle, heave and total resistance caused by ship response due to interceptor installation. This study aims to predict ship resistance due to interceptor installation. Thus, this research becomes the initial design to analyze the interceptor design on highspeed vessel.

In our research, we focus on the performance of CFD by comparing experimental methods [18]. The difference from previous research is the object of research. Keep in mind that each ship has different characteristics, especially for fast boats. This study uses a planing hull ship model, namely the Aragon 2 ship without an interceptor and with an interceptor. Changes in the interceptor stroke were observed at 60% and 100% heights. The CFD results also prove that CFD can simulate well and the interceptor is proven to improve ship performance.

2. Methods
2.1. Hull details

This study uses a numerical simulation method based on the finite volume method to predict the motion and resistance of the ship. The object of research is using the Aragon 2 ship which is included in the category of planing hull ship. The Aragon 2 ship as depicted in Figure 1 with the main dimensions in Table 1 has been experimentally tested by Park et al with the interceptor dimensions that have been adjusted to the ship's geometry [18]. The data is redrawn using 3D modeling with the NURBS approach. The numerical analysis approach uses ITTC standards to simplify the work. Visualization of the position of the interceptor can be seen in Figure 2. The interceptor stroke is commonly called the interceptor height. The interceptor is controlled using a hydraulic motor, so its height can be changed according to the speed of the ship. The interceptor height is 0%, 60%, 100% i.e. 0 mm, 30 mm, 50 mm.
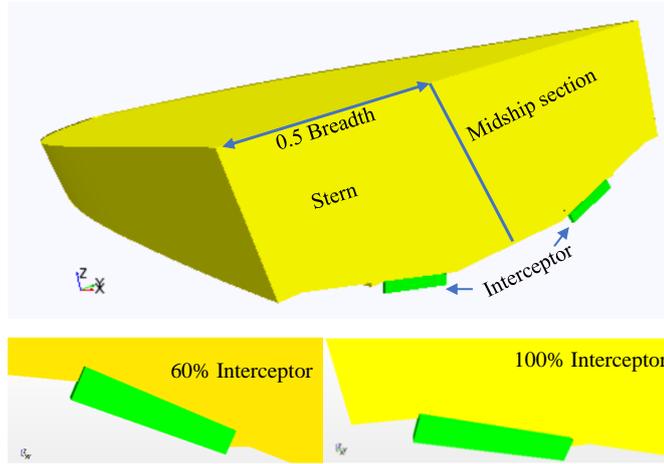

Figure 1. Aragon-2 [18]

Figure 2. Interceptor Configuration

Table 1. Main Dimension of Aragon-2 and Interceptor [18]

Main dimension	Prototype	Experiment scale 1 : 5.33	Unit
Length overall (LOA)	8000	1500	mm
Length waterline (LWL)	7539	1414	mm
Breadth overall	2300	431	mm
Draft	445	83	mm
Weight	3000	19.77	Kg
Interceptor height (hi) (100%)	50	9.37	mm
Interceptor span (s)	300	56.25	mm
Chine breadth	2200	412.75	mm
C.G. from transom (LCG)	2647	496	mm
C.G. from baseline (KG)	761	14.2	mm
Deadrise angle		16 at transom, 24 at midship	degree

2.2. Numerical procedure

It is assumed that the fluid is viscous and Newtonian. The problem domain is thought to consist of two phases, namely air and water (denoted by the letters a and w, respectively). The substance is designed to be incompressible. Using the Eulerian technique, the conservation equations fluid motion are developed [19]:

$$\nabla . u = 0$$
$$\partial_t(\gamma) + \nabla . (u\gamma) = 0$$
$$\partial_t(\rho_c u) + \nabla . (\rho_c u)u^T = -\nabla_p + \nabla . (\mu_c + \mu_t)[\nabla_u + \nabla_u{}^T] + \rho_c f_b$$

Where u is the velocity vector of the flow, ρ_c is the density of the flow, μ_c refer to viscosity at any point. p is the pressure and f_b = (-g 0 0) represent the external forces set in from gravity. γ is the phase fraction of the fluid with values start from 0 to 1 to identified air and water condition. μ_c is the compound of viscousity and μ_t is the eddy viscosity. Two different phases include water (w) and air (a). This research was conducted by numerical simulation method. To ensure the accuracy of numerical research procedures, ITTC is used as a standard for conducting numerical tests. Some of the ITTC recommendations included in this study are [20]:

1. Virtual computational domain
2. Time-step
3. Convergence
4. Mesh Study
5. y+ mesh spacing

Figure 3a is a towing tank from an experimental study conducted by Park et al. Meanwhile Figure 3b visualizes the boundary conditions and computational domain modeled as a towing tank in a numerical simulation. The length of the domain is 1 L from the ship's bow position to the inlet and 2.5 L from the ship's stern to the outlet. The width of the background is 1.5 L and the overall length is 4.5 L. The height of the background is 3 L with the bottom of the ship 2 L from the bottom of the background. It is known that L is the perpendicular length of the ship. The pressure outlet is used to review the static pressure due to static pressure. The ship is modeled in symmetry so that only half of the hull is analyzed to reduce computation time.

This study defines the movement of the ship with Dynamic Fluid Body Interaction (DFBI) using two degrees of freedom, free heave and trim. The overset area that moves with the ship allows the ship to translate trim and heave. Meanwhile the background area is set in a static state. The translational and rotational motion at the center of mass of the ship model uses trim and heave as described in equations 1 and 2 below:

$$M \frac{d}{dt} \omega = n \tag{1}$$

and

$$m \frac{dv}{dt} = f \tag{2}$$

Where M is the x-axis rotation's moment of inertia and n is the resultant moment of the ship model acting on the axis rotation. ω is the ship's angular velocity about the y-axis. m is the mass of the ship. f is the resultant force acting on the surface of the ship and v is the speed of the ship. The fluid pressure and shear force on each surface of the ship are used to calculate the subsequent forces and moments operating on it. We have also added supporting references to this study. Panahi et al. has conducted extensive study into this topic [21].

(a)   (b)
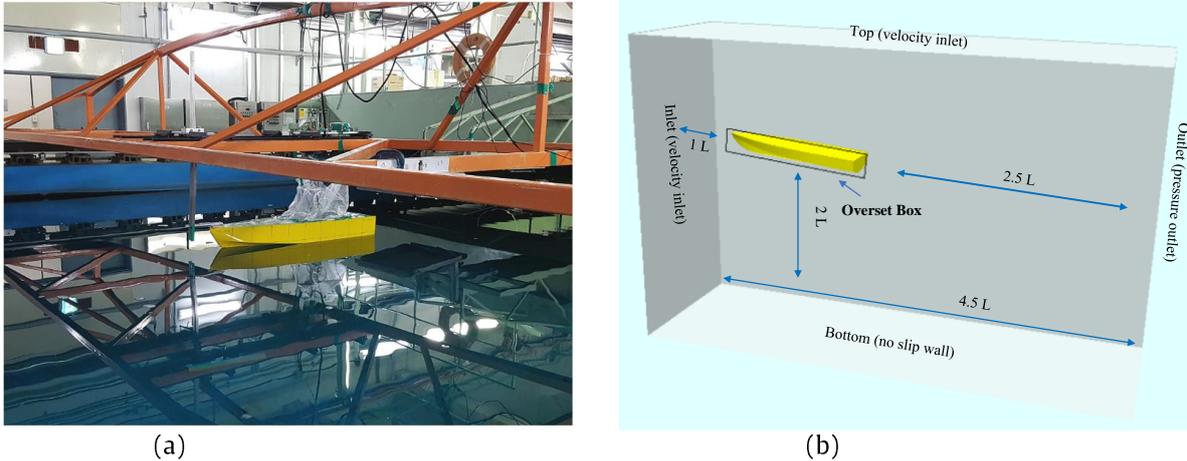
Figure 3. (a) Experimental Study by Park et al. [18], (b) Numerical Simulation

Figure 4 describes the different mesh density distributions. Density mesh will be more detailed in the ship area and areas that have the potential for translation of physical properties related to ship motion. The density of the mesh in the background is not too small so that it can reduce the computation time. Mesh density can also be a determinant of the success of donor acceptor cells, so it is important to recognize and examine the characteristics of the research object. This study applies the overset mesh technique with the working principle of donor acceptor cells. This technique needs more than one geometry, with the background acting as the giver and the overset acting as the beneficiary of the donation. At each end of the geometry in the overset, active cells serve as a bridge between donor and acceptor cells.

The reason for using this technique has also been studied in research on the comparison between the overset and moving mesh methods [22]. In the following year, research on the comparison between moving mesh and morphing mesh techniques showed a better level of accuracy than morphing mesh [23]. Despite getting a good level of accuracy, the overset mesh method takes a long time to calculate the results due to the interaction between the mesh geometries. In the overset mesh technique, the equation is solved independently in the two locations, and the result is interpolated in the overlapped area made up of cells referred to as donors and acceptors where data is exchanged. Although a linear interpolation approach needs more computer work than other alternatives, it is employed because it minimizes interpolation errors and ensures greater convergence and an accurate answer.

One of the parameters to guarantee CFD accuracy is Y+ (wall function). To represent boundary layer phenomena using dimensionless units, the value of y+ is used. The ITTC suggests that y+ be valued at 30 y+ 100. This study demonstrates that the value of y+ can range from 40 to 60, as shown in Figure 5.

The time step is the iteration interval period. This research uses CFL (Courant-Friedrichs Lewy). CFL is used to represent the quantity of points traveled by fluid particles in a certain time interval. This study uses a time step of 0.008s as described in Figure 6.

This research applies a grid independence study to select the most suitable mesh quantity for each simulation. There are five grids with a mesh quantity of 0.52; 0.66; 0.87; 1.24; 1.47 in million cells. From this analysis, convergent results were obtained on each grid, but grids 4 and 5 showed the best convergence results as described in Figure 7a. By reviewing the elapsed time in Figure 7b, grid number 4 is chosen because the time is more effective and all values have been declared convergent. For comparison of trim, drag and heave values can be observed in Figure 8.
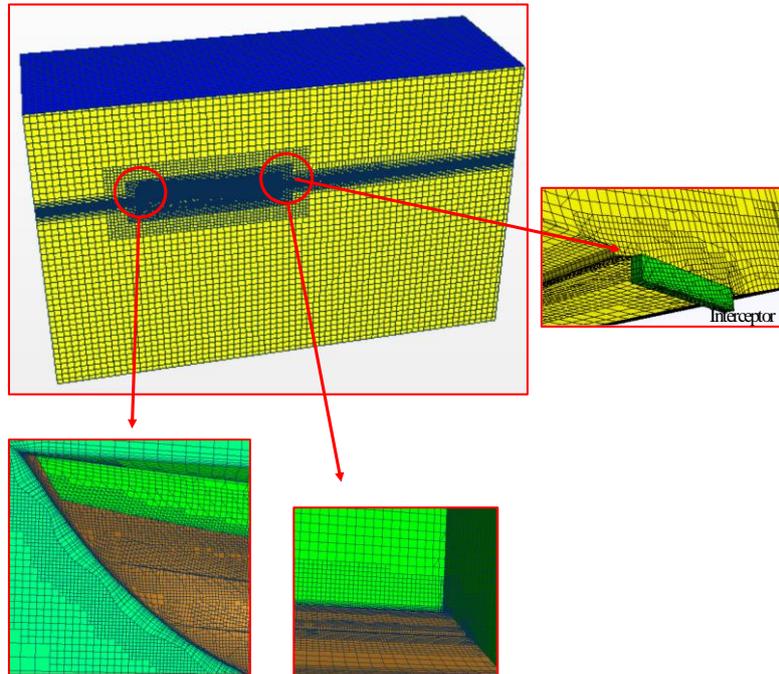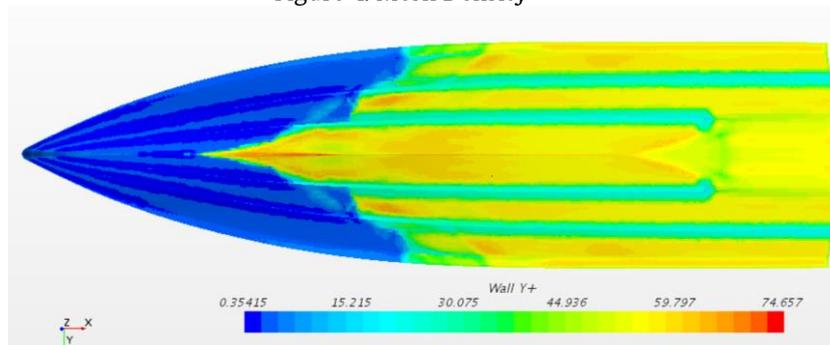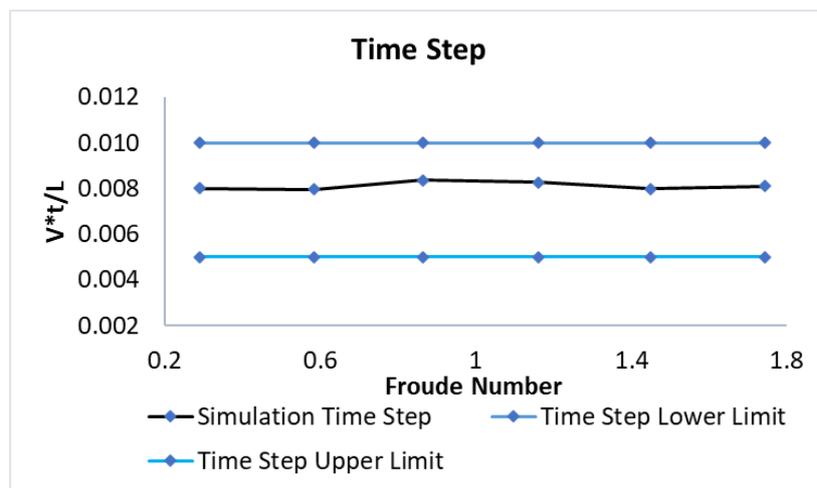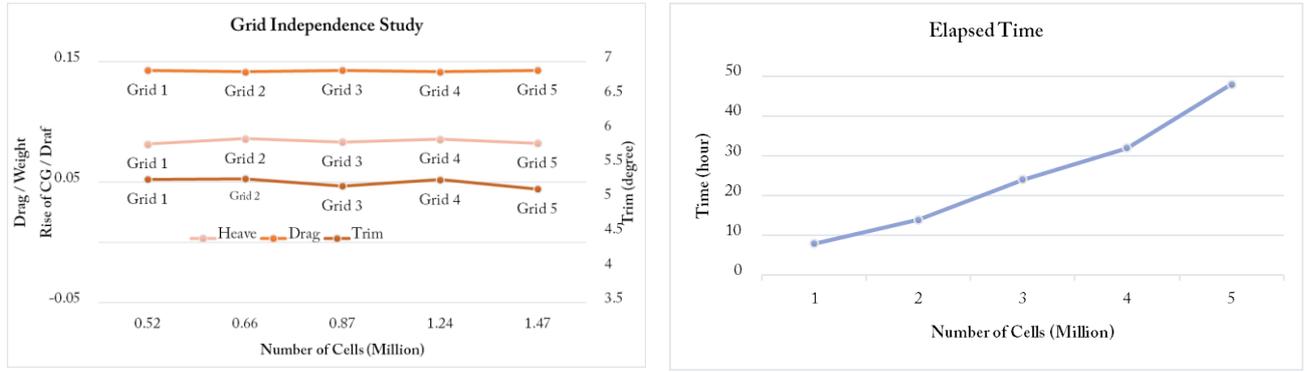
Figure 4. Mesh Density

Figure 5. y+

Figure 6. Time Step

(a)

(b)

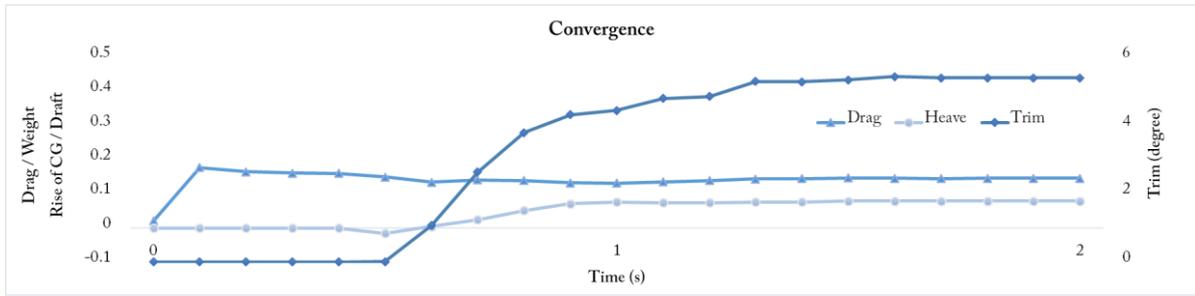Figure 7. (a) Grid Independence Study, (b) Elapsed Time

Figure 8. Convergence

3. Result and Discussion

The experimental study by Park et al. used as comparison data for CFD validation. The trim, heave and drag values show the same pattern between CFD and experiment. Figure 9 shows that the CFD method can simulate well. Figure 9 a, b, and c shows the calculation underpredicts gap of 7.5% to 9.9%. The ship experienced an increase in the value of drag at 100% interceptor at Froude number 1.45 with an experimental value of 0.22 and a CFD value of 0.2. In the drag with 60% interceptor there is an underpredicts drag in the experimental analysis with the number 0.21 and using CFD the results are 0.19 at the Froude number 1.45. At low speeds the increase in total drag is still visible because the resistance due to the interceptor is greater than the reduction in drag due to the hydrostatic position of the ship. But at high speeds there is a significant reduction in drag. This is also in line with the research of Salian and Brizzola [24].
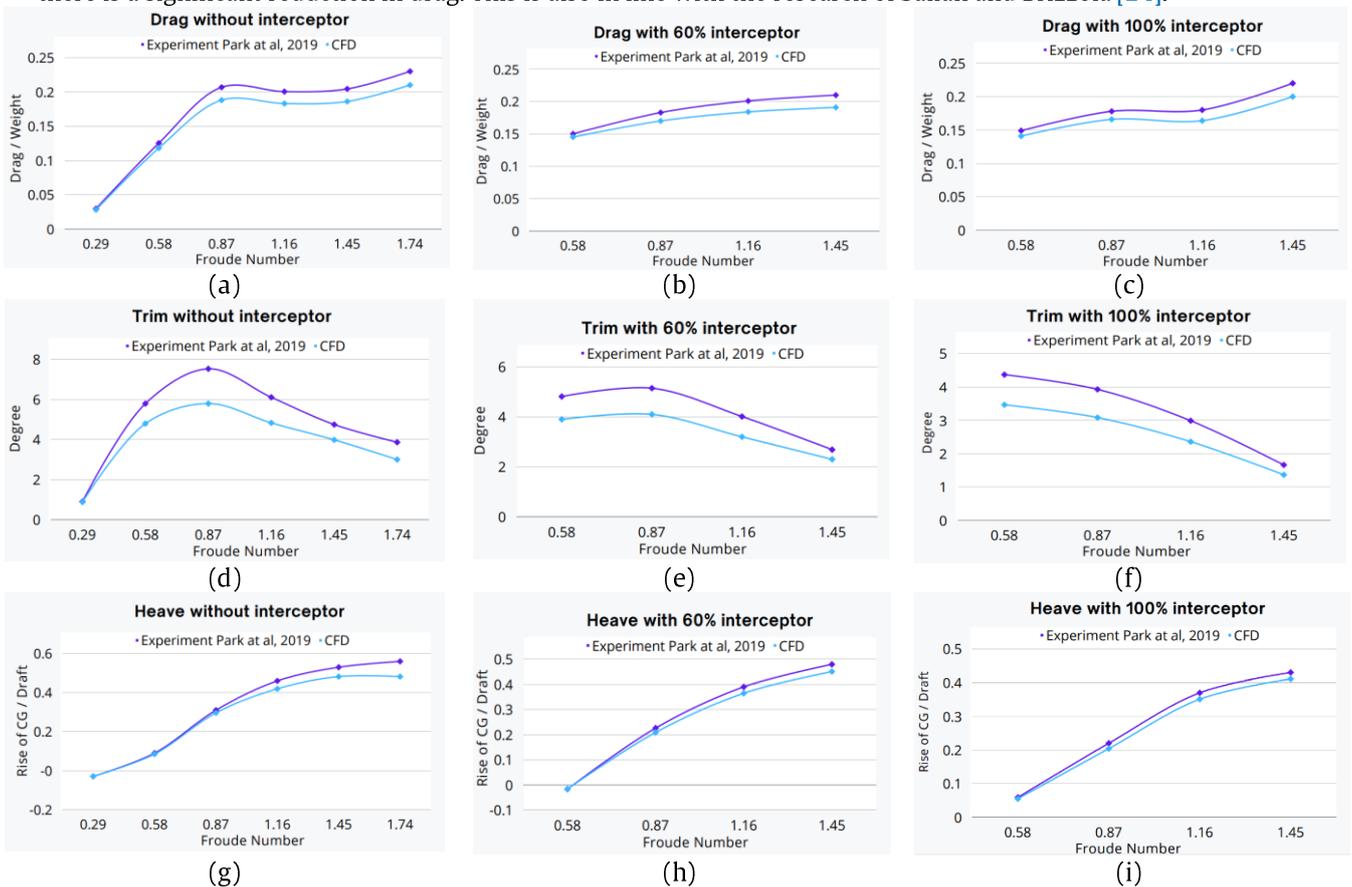

(a)

(b)

(c)

(d)

(e)

(f)

(g)

(h)

(i)

Figure 9. Verification Result

Table 2. Percentage of difference between Experiment [18] and CFD results

Fn	Percentage of difference between Experiment [18] and CFD results (%)								
	0% interceptor			60% interceptor			100% interceptor		
	Drag	Heave	Trim	Drag	Heave	Trim	Drag	Heave	Trim
0.29	6.1	3.2	0.9	-	-	-	-	-	-
0.58	7.5	4.6	7.5	3.4	4.6	8.4	3.4	7.3	6.3
0.87	9.9	5.7	10.7	7.6	8.3	9.2	7.6	7.8	9.8
1.16	9.5	9.6	9.5	9.2	7.0	9.1	9.2	5.4	9.6
1.45	9.9	9.8	6.9	9.9	6.3	6.0	9.9	7.3	7.8
1.74	9.5	10.0	7.4	-	-	-	-	-	-

The CFD data, which were calculated using interceptor, are seen to correspond to the experimental data. Figure 9 d, e, and f shows CFD data with trim errors ranging from 9.27% to 10.7%. The highest trim value is at the Froude number 0.87 with the experimental value at 7.5 deg and with the CFD method the number is 5.8 deg. At 100% interceptor, the highest trim on the Froude number is 0.58 which shows the experimental value is at 4.37 deg while the CFD simulation is at 3.4 deg. From the graph it is clear that the interceptor produces a decrease in trim across the tested speed range. The reduction in trim indicates a bow down movement of the hull trim which is generally characterized by a decrease in drag.

Figure 9 g, h, and i shows the range of error heave values between 5.7% and 10%. Ships without an interceptor on the Froude number 1.45 with an experimental value of 0.53 and a CFD simulation obtained 0.48. The ship has improved the heave value at 100% interceptor condition with the Froude number 1.45 resulting in the experimental value being at 0.43 and the CFD simulation obtained 0.41. At 60% interceptors in the Froude number 1.45, the heave value reduction was obtained using experimental analysis with a value of 0.48 and in the CFD simulation it was obtained 0.45. The interesting thing to consider is that as speed increases, heave mistakes get worse.

This study found a difference in the results of the analysis between CFD and experiment of up to 10.7%, shown on the trim graph at the Froude number 0.87. A complete analysis of the gap between CFD calculations and experiments in this study can be seen in Table 2. Due to the limitations of CFD in modeling the environment according to real conditions, CFD calculations have gaps that do not match the experimental results. Brizzola and Serra investigated the accuracy of the CFD experiment. The study presents a detailed configuration of the CFD model including mesh type, resolution, boundary conditions and turbulence model. The research results found that CFD can verify experimental results with a tolerance of 10% [14].
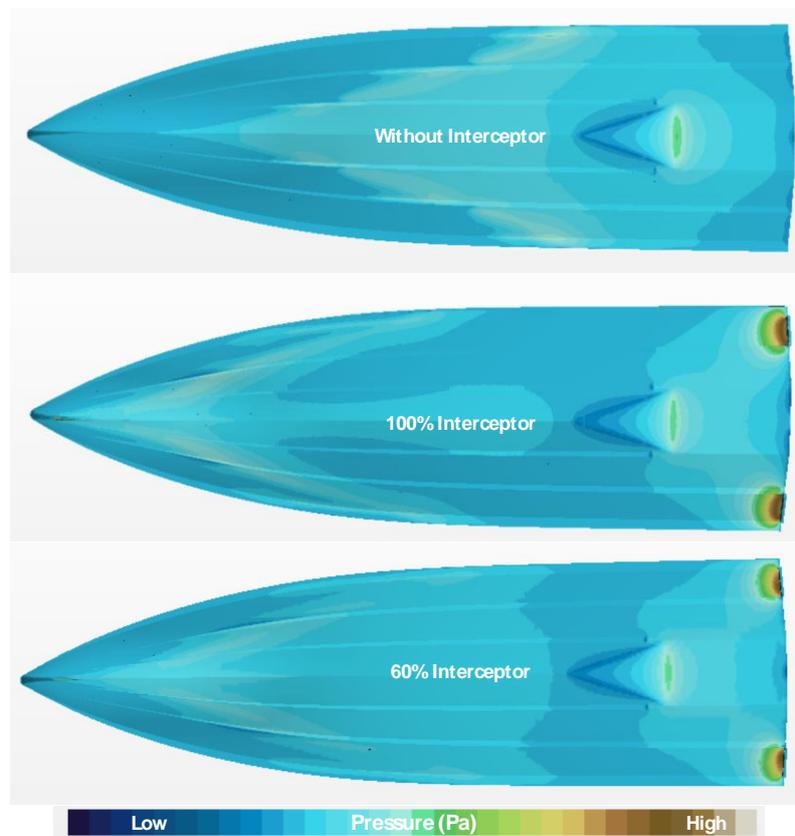

Figure 10. Pressure Distribution

The pressure contribution acting on the vessel's bottom is measured. The tested information corresponds to the time at which the vessel achieved dynamic equilibrium. The pressure distribution on the bottom of the ship can be seen

in Figure 10. Observations indicate that an increase in velocity results in an increase in pressure at the stagnation line. The figure provides a visualization of the effect of the pressure generated with and without the interceptor on the Froude number 1.74. without using an interceptor, the ship's pressure will be concentrated on the bottom of the ship. Meanwhile, the use of an interceptor causes a pressure distribution that is centered on the stern area of the ship, namely the interceptor position. The height of the interceptor also greatly affects the size of the resulting pressure. At 100% interceptor creates greater pressure than 60% interceptor. This is because the interceptor works by cutting the flow at the bottom of the ship so that a discontinuity of flow is formed which directly affects the increase in pressure in that area.

The pressure generated by the interceptor is closely related to the trim of the ship as observed through the volume fraction of water in Figure 11. The application of the interceptor can reduce trim on the bow of the ship. This phenomenon is supported by the moment generated by the interceptor due to the pressure generated by the interceptor. The interceptor moment can balance the bow moment of the ship so that this condition can change the trim angle of the ship and even cause the ship to be in an even keel condition. Ships using interceptors at Froude 1.74 will result in excessive trim. When installing the interceptor on Froude 1.74, the ship experienced negative trim due to excessive interceptor moment and was declared an unfit interceptor. However, the interceptor is still suitable for use at the same Froude number if it is 60% high. Mansoori and Fernandes stated that if the moment generated by the interceptor is smaller than the trim moment, then the interceptor efficiency is weak, but if the moment generated by the interceptor is greater than the trim moment then the interceptor cannot be used. An inefficient interceptor has poorly controlled ship trim, while an unsuitable interceptor can cause negative trim while increasing the ship's drag [25].

The application of the interceptor also affects the wave pattern that is formed as described in Figure 12. The wave pattern is the interaction of waves in the hull area of the ship. From the simulation results, the wave pattern shows the distribution of pressure and wave elevation between the hull with and without the interceptor. Changes in wave patterns (characteristics) are also affected by the height of the interceptor. The higher the interceptor used, the greater the pressure and elevation of the wave formed. This is due to disturbances in flow velocity and pressure due to the interaction effect of waves and interceptors.

Overall, the results of this study are in line with the experimental studies of Park et al [18]. Verification was declared successful with a research gap tolerance of 10.7%. In addition, the use of interceptors can improve the performance of the ship's planing hull. This is evidenced by the improvement and reduction of drag, heave and trim. The following study on interceptors is also in line with Mansoori and Fernandes' study of interceptors on high-speed craft ships through numerical simulations. In this study, it was found that using an interceptor could increase the pressure and lift force at the stern of the ship while reducing the trim angle [26].
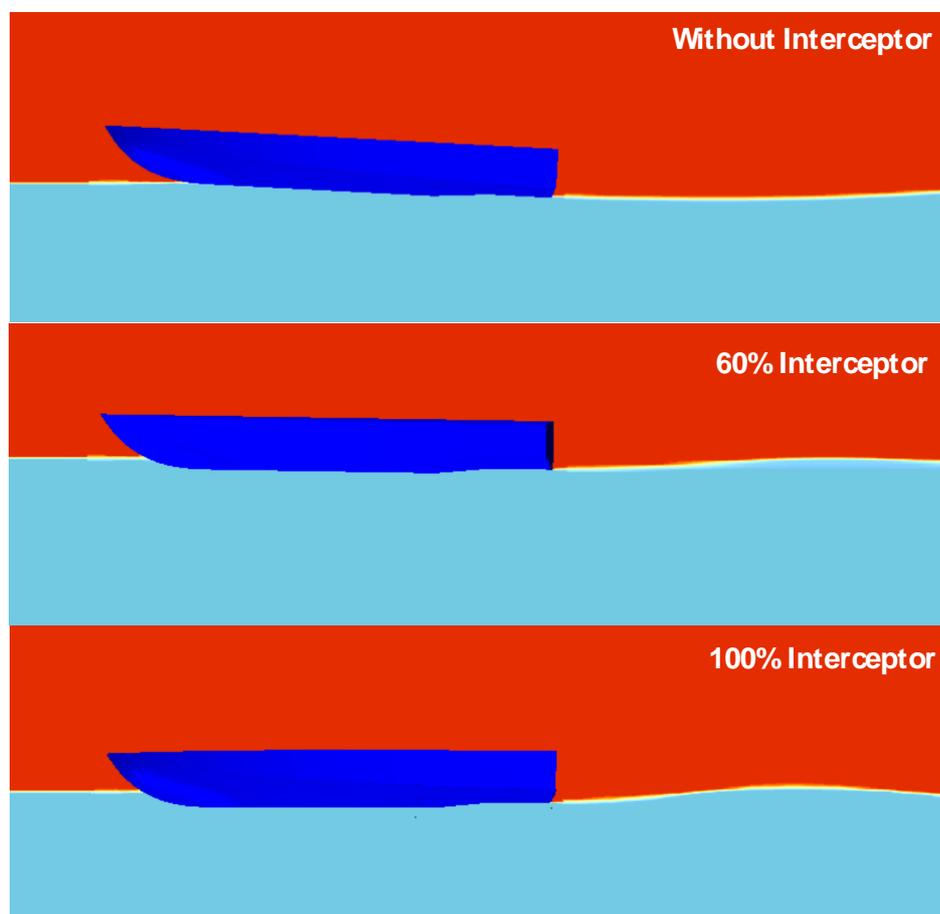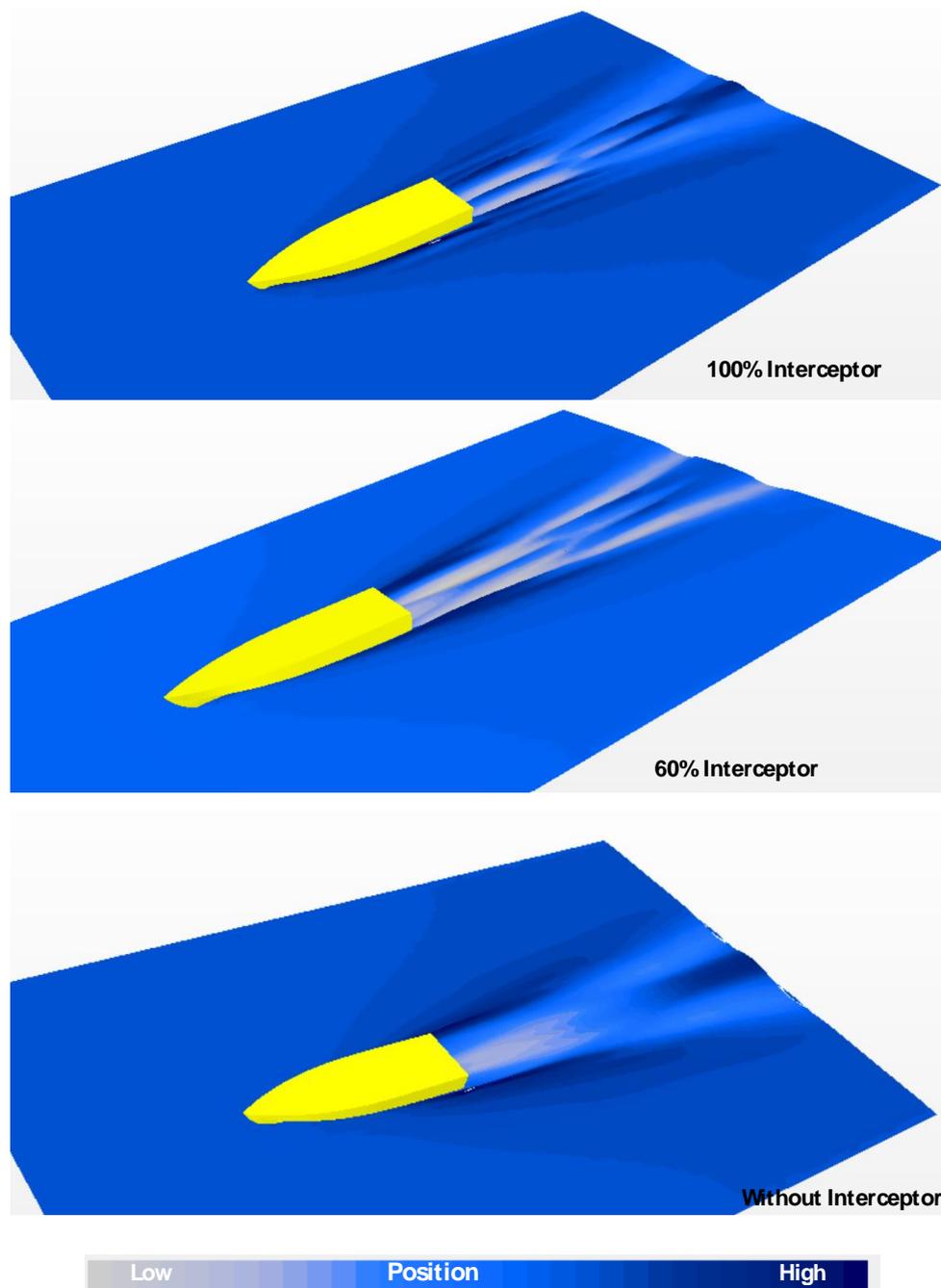

Figure 11. Volume Fraction of Water

Figure 12. Wave Pattern

4. Conclusion

The simulations shown in this paper were carried out to enhance our understanding of the precision and capability of CFD simulations in numerical of high-speed planing concern. In this study, it was found that the numerical simulation corresponds to the experimental data with error percentages is 10.7%. This can be achieved by carrying out several ITTC recommendations and grid independence studies related to numerical simulations. The overset method provides a higher level of precision in calculating the total drag and running attitudes of a high-speed vessel. This study explains that CFD is able to perform calculations on high-speed vessel with the addition of an interceptor and it is known that interceptors are able to improve ship performance. This study also proves that stroke of the interceptor can affect the performance of the planing hull ship. This can be observed by reviewing the pressure, the condition of the vessel by visualizing the volume fraction of water, as well as the wave pattern that is formed.

References

[1]   D. Savitsky, " Hydrodynamic design of planing hulls," *Marine Technology and SNAME*, vol. 1, no. 1, pp. 71– 95, 1964.

[2]   H. Jokar, H. Zeinali, and M. H. Tamaddondar, " Planing craft control using pneumatically driven trim tab," *Mathematics and Computers in Simulation*, vol. 178, pp. 439– 463, 2020, doi: 10.1016/j.matcom.2020.05.032.

[3]   A. A. K. Rijkens, H. M. A. Cleijsen, and J. A. Keuning, " On the hydrodynamic performance of an improved motion control device for fast ships," *FAST 2013 - 12th International Conference on Fast Sea Transportation*, 2013.

[4]   M. Mansoori and A. C. Fernandes, " Interceptor and trim tab combination to prevent interceptor's unfit effects,"

Ocean Engineering, vol. 134, 2015, pp. 140– 156, 2017, doi: 10.1016/j.oceaneng.2017.02.024.

[5]   M. Mansoori and A. C. Fernandes, " The interceptor hydrodynamic analysis for controlling the porpoising instability in high speed crafts," *Applied Ocean Research*, vol. 57, pp. 40– 51, 2016, doi: 10.1016/j.apor.2016.02.006.

[6]   S. Jangam and P. Sahoo, " Numerical investigation of interceptor effect on seakeeping behaviour of planing hull advancing in regular head waves," *Brodogradnja*, vol. 72, no. 2, pp. 73– 92, 2021, doi: 10.21278/brod72205.

[7]   M. H. Karimi, M. S. Seif, and M. Abbaspoor, " An experimental study of interceptor' s effectiveness on hydrodynamic performance of high-speed planing crafts," *Polish Maritime Research*, vol. 20, no. 2, pp. 21– 29, 2013, doi: 10.2478/pomr-2013-0013.

[8]   D. Savitsky and P. Ward Brown. "Procedures for hydrodynamic evaluation of planing hulls in smooth and rough water." Marine Technology and SNAME News 13.04 (1976): 381-400.

[9]   D. J. Kim, S. Y. Kim, Y. J. You, K. P. Rhee, S. H. Kim, and Y. G. Kim, " Design of high-speed planing hulls for the improvement of resistance and seakeeping performance," *International Journal of Naval Architecture and Ocean Engineering*, vol. 5, no. 1, pp. 161– 177, 2013, doi: 10.2478/ijnaoe-2013-0124.

[10]   R. Yousefi, R. Shafaghat, and M. Shakeri, " Hydrodynamic analysis techniques for high-speed planing hulls," *Applied Ocean Research*, vol. 42, pp. 105– 113, 2013, doi: 10.1016/j.apor.2013.05.004.

[11]   Samuel, M. Iqbal, and I. K. A. P. Utama, " An investigation into the resistance components of converting a traditional monohull fishing vessel into catamaran form," *International Journal of Technology*, vol. 6, no. 3, pp. 432– 441, 2015, doi: 10.14716/ijtech.v6i3.940.

[12]   Samuel, D. J. Kim, M. Iqbal, A. Bahatmaka, and A. Rio Prabowo, " Bulbous bow applications on a catamaran fishing vessel for improving performance," in *MATEC Web of Conferences*, 2018, vol. 159, pp. 1– 6, doi: 10.1051/matecconf/201815902057.

[13]   O. F. Sukas, O. K. Kinaci, F. Cakici, and M. K. Gokce, " Hydrodynamic assessment of planing hulls using overset grids," *Applied Ocean Research*, vol. 65, pp. 35– 46, 2017, doi: 10.1016/j.apor.2017.03.015.

[14]   S. Brizzolara and F. Serra, " Accuracy of CFD codes in the prediction of planing surfaces hydrodyamic characteristics," *The 2nd International Conference on Marine Research and Transportation*, no. June 2007, pp. 147– 158, 2007, [Online]. Available: http://www.icmrt07.unina.it/Proceedings/Papers/B/14.pdf.

[15]   A. Hay, A. Leroyer, and M. Visonneau, " H-adaptive Navier-Stokes simulations of free-surface flows around moving bodies," *Journal of Marine Science and Technology*, vol. 11, no. 1, pp. 1– 18, 2006, doi: 10.1007/s00773-005-0207-0.

[16]   Samuel, D. J. Kim, A. Fathuddiin, and A. F. Zakki, " A Numerical Ventilation Problem on Fridsma Hull Form Using an Overset Grid System," *IOP Conference Series: Materials Science and Engineering*, vol. 1096, no. 1, p. 012041, 2021, doi: 10.1088/1757-899x/1096/1/012041.

[17]   M. P. Wheeler, K. I. Matveev, and T. Xing, " Validation study of compact planing hulls at pre-planing speeds," *American Society of Mechanical Engineers, Fluids Engineering Division (Publication) FEDSM*, vol. 2, pp. 1– 8, 2018, doi: 10.1115/FEDSM2018-83091.

[18]   J. Y. Park *et al.*, " An experimental study on vertical motion control of a high-speed planing vessel using a controllable interceptor in waves," *Ocean Engineering*, vol. 173, pp. 841– 850, 2019, doi: 10.1016/j.oceaneng.2019.01.019.

[19]   A. Hosseini, S. Tavakoli, A. Dashtimanesh, P. K. Sahoo, and M. Kõrgesaar, " Performance prediction of a hard-chine planing hull by employing different cfd models," *Journal of Marine Science and Engineering*, vol. 9, no. 5, 2021, doi: 10.3390/jmse9050481.

[20]   ITTC, " Practical Guidelines for Ship CFD Applications," *ITTC – Recommended Procedures and Guidelines ITTC*, pp. 1– 8, 2011.

[21]   R. Panahi, E. Jahanbakhsh, and M. S. S. Ã, " Towards simulation of 3D nonlinear high-speed vessels motion," vol. 36, pp. 256– 265, 2009, doi: 10.1016/j.oceaneng.2008.11.005.

[22]   F. De Luca, S. Mancini, S. Miranda, and C. Pensa, " An extended verification and validation study of CFD simulations for planing hulls," *Journal of Ship Research*, vol. 60, no. 2, pp. 101– 118, 2016, doi: 10.5957/JOSR.60.2.160010.

[23]   A. De Marco, S. Mancini, S. Miranda, R. Scognamiglio, and L. Vitiello, " Experimental and numerical hydrodynamic analysis of a stepped planing hull," *Applied Ocean Research*, vol. 64, no. 13 Februrary, pp. 135– 154, 2017, doi: 10.1016/j.apor.2017.02.004.

[24]   R. Salian and S. Brizzolara, " Adjustable energy saving device for transom stern hulls," *SNAME Maritime Convention, SMC 2018*, 2018.

[25]   M. Mansoori, A. C. Fernandes, and H. Ghassemi, " Interceptor design for optimum trim control and minimum resistance of planing boats," *Applied Ocean Research*, vol. 69, pp. 100– 115, 2017, doi: 10.1016/j.apor.2017.10.006.

[26]   M. Mansoori and A. C. Fernandes, " The interceptor hydrodynamic analysis for controlling the porpoising instability in high speed crafts," *Applied Ocean Research*, vol. 57, pp. 40– 51, 2016, doi: 10.1016/j.apor.2016.02.006.